An Analytical and Experimental Study of a Control System's Sensitivity to Structural Modifications

Raphael T. Haftka,* Zoran N. Martinovic,† William L. Hallauer Jr.,* and George Schamel†
Virginia Polytechnic Institute and State University, Blacksburg, Virginia

Two aspects of the sensitivity of a control system to minor structural modifications are discussed. The first is the sensitivity of the performance of the control system, which is usually associated with the robustness of the system. The second is the sensitivity of the optimum design of the control system, which is important in the assessment of the need for combined control/structural design. The two aspects of sensitivity are demonstrated for a flexible laboratory structure controlled by several rate-feedback colocated force-actuator velocity-sensor pairs. Both the performance and the optimum design of the control system are shown to be quite sensitive to structural modifications. Analytical predictions of sensitivity are validated experimentally.

Nomenclature

C = damping matrix ($n_n \times n_n$)
c = vector of control gains
c_i = ith viscous damping coefficient or control gain
f = performance index
g_j = jth constraint in an optimization problem
j = $(-1)^{1/2}$
K = stiffness matrix ($n_n \times n_n$)
M = mass matrix ($n_n \times n_n$)
m_k = kth lumped mass
N = matrix defined following Eq. (1)
n_c = number of sensor-actuator pairs
n_g = number of constraints in control optimization problem
n_n = number of structural degrees of freedom
p = vector of structural parameters
p_0 = vector of structural parameters in baseline design
r = mode number
u = displacement vector ($n_n \times 1$)
x = vector of control system design variables
y = vector of sensor-actuator locations
y_i = location of the ith sensor-actuator pair
μ_r = rth pair of eigenvalues defined in Eq. (3)
λ_j = jth Lagrange multiplier
ω_r = imaginary part of rth eigenpair defined in Eq. (3)
σ_r = real part of rth eigenpair defined in Eq. (3)
ζ_r = damping ratio of rth eigenpair defined in Eq. (4)

I. Introduction

LARGE space structures will face difficult problems of vibration control. Because of the requirement for low weight, such structures will probably lack the stiffness and damping required for adequate passive control of vibrations. Therefore, a great deal of research has been conducted recently on designing active control systems for such structures.

Very recently, there has been considerable interest in simultaneous design of the structure and the control system so as to produce a truly optimum configuration (e.g., Refs. 1-4). Before one embarks on such an ambitious undertaking, it is important to determine that there is a synergistic effect in designing a structure and a control system simultaneously. Several recent works (e.g., Refs. 5 and 6) approached the problem indirectly, by showing that the performance of the control system may be enhanced by optimizing the structure to improve a structural performance index such as the overall stiffness or a vibration frequency. Reference 7 approached the question of the possible synergistic effect more directly by showing that minor structural modifications can have a large effect on control system performance. It also demonstrated how the magnitude of the synergistic effect can be predicted from a sensitivity analysis of the control system performance.

The work of Ref. 7 was limited to the sensitivity of a given control system to minor structural modifications. This paper extends that work by assuming that the control system is *optimized* for maximum performance for the original structural configuration, and then *reoptimized* to take full advantage of the structural modifications. Sensitivity analysis of optimized systems is used to predict the changes required in the control system to take full advantage of the structural modifications, and the ensuing change in performance. Additionally, this paper examines the possible adverse effects of minor structural modifications on the performance of the control system. This question of the sensitivity (or, conversely, the robustness) of the control system with respect to changes and errors in the structural model has received much attention (e.g., Refs. 8-10) and is considered crucial in practical applications. Sensitivity calculations are carried out analytically and validated experimentally for a flexible cruciform beam supported by cables.

II. Design Optimization and Sensitivity

It is assumed that a control system is designed for a structure characterized by a vector p of structural parameters. The control system design is assumed to be a solution of an optimization problem of the following form:

find x
to minimize $f(x, p)$
subject to some constraints
$g_j(x, p) \geq 0, \quad j = 1, \ldots, n_g$

Presented as Paper 85-0807 at the AIAA/ASME/ASCE/AHS 26th Structures, Structural Dynamics and Materials Conference, Orlando, FL, April 15-17, 1985; received May 17, 1985; revision submitted June 11, 1986. This paper is declared a work of the U.S. Government and is not subject to copyright protection in the United States.

*Professor, Department of Aerospace and Ocean Engineering. Member AIAA.

†Graduate Research Assistant, Department of Aerospace and Ocean Engineering. Student Member AIAA.

where x is a vector of control system design variables, and $g_j(x, p)$ represents behavioral constraints (such as stability limits) or side constraints (such as limits on gains). The particular form of the preceding optimization formulation for rate-feedback control is given in Secs. III and V. The solution $x^*(p_0)$ of the optimization problem for a nominal structure characterized by $p = p_0$ is called the baseline design. We are interested in the sensitivity of the baseline design to structural modifications, i.e., to changes in the vector p.

Two types of sensitivity may be considered. The first is the sensitivity of the baseline design to structural modifications when the control design x^* is frozen. This type of sensitivity is a measure of the robustness of the design and is given by the partial derivatives

$$\frac{\partial f}{\partial p_k}(x^*, p_0) \qquad \frac{\partial g_j}{\partial p_k}(x^*, p_0)$$

where p_k is a component of p.

The second type of sensitivity derivative measures the change in the optimum design of the control system as the structure is modified. Denoting $f^* = f(x^*, p)$, we are interested in the derivatives $\partial x^*/\partial p_k$ and $\partial f^*/\partial p_k$. For the case where the number of active constraints is equal to the number of design variables,[11]

$$\frac{\partial x^*}{\partial p_k} = -(N^T)^{-1}\frac{\partial g_a}{\partial p_k} \tag{1}$$

where the matrix N has components $n_{ij} = \partial g_{aj}/\partial x_i$. The vector g_a consists of constraints g_{aj}, which are active [that is, $g_{aj}(x^*, p_0) = 0$] for the baseline design. Similarly, the change in optimized performance is

$$\frac{\partial f^*}{\partial p_k} = \frac{\partial f}{\partial p_k} - \sum_{j=1}^{n_g} \lambda_j \frac{\partial g_j}{\partial p_k} \tag{2}$$

where λ_j are Lagrange multipliers obtained at the optimum design of the control system.

The sensitivity of the optimum control design is a measure of the interaction between the design of the structure and the design of the control system. Large values of $\partial f^*/\partial p_k$ indicate that there is a potential for enhancing the control system performance by minor structural modifications.

III. Rate Feedback Control

The control system selected for the present study is based on rate feedback control produced by pairs of colocated velocity sensors and actuators. This simple control method was used rather than a more involved method, such as optimal or modal control, because experimental validation was a primary objective and the authors had available a proven analog rate feedback control system.[7] In contrast, most experimental implementations of more involved methods (e.g., Refs. 12 and 13) have encountered substantial difficulty in simply achieving stable control systems, let alone validating theoretical models. The colocated pairs of sensors and actuators act as electromagnetic dashpots, and the control design variables are the feedback gains c_i, $i = 1, \ldots, n_c$, and the locations y_i of the sensor-actuators pairs. Following Ref. 14, the objective function for the control system design is the sum of the gains Σc_i, and constraints are placed on the eigenvalues of the closed-loop system to ensure adequate stability. The stability of the system is determined by the n_n possible pairs of complex conjugate eigenvalues μ_r, $r = 1, 2, \ldots, n_n$,

$$\mu_r = \sigma_r \pm j\omega_r, \qquad j = (-1)^{1/2} \tag{3}$$

In particular, in the present investigation the measure of stability is the modal damping ratio ζ_r:

$$\zeta_r = -\sigma_r/\left(\sigma_r^2 + \omega_r^2\right)^{1/2} \tag{4}$$

The control optimization problem now becomes

$$\begin{aligned} &\text{find } x^T = [c^T, y^T] \\ &\text{to minimize } f(x, p) = \sum_{i=1}^{n_c} c_i \\ &\text{subject to} \\ &g_j(x, p) = \zeta_j - \zeta_{LW} \geqq 0, \qquad j = 1, \ldots, n_m \\ &\text{and} \qquad c_i \geqq 0, \qquad i = 1, \ldots, n_c \end{aligned} \tag{5}$$

where ζ_{LW} is minimum required damping ratio.

Although the sum of gains Σc_i has questionable value as a practical control performance index, it was selected because it is simple and compatible with rate feedback control. Use of this simple objective function was helpful in both development of the methods presented herein and research currently in progress on more practical objective functions based on control gains.

Because of the simple form of the objective function, the term "optimized" is used herein (rather than the more common "optimal") in referring to the control system that is obtained by performing the optimization process.

IV. Cruciform Beam Model

The procedure described in the previous section has been applied to a small laboratory structure. The structure consists of a vertical beam and an attached horizontal crosspiece, with the vertical beam suspended by cables in tension at its top and bottom (Fig. 1). The crosspiece was designed so that the structure would have third and fourth vibration modes with relatively close natural frequencies. The vertical beam is a uniform steel beam 80 in. (2.03 m) long, with a rectangular cross section $2 \times \frac{1}{8}$ in. (51×3.2 mm). The crosspiece is an aluminum beam 32 in. (0.81 m) long, with a rectangular cross section $2 \times \frac{1}{8}$ in. (51×3.2 mm). Small masses consisting of two ceramic magnets are located at both ends of the crosspiece, which is secured to the vertical beam by a clamp. The vertical beam is attached to the floor and ceiling by four 0.09-in. (2.3-mm)-diam steel cables, as shown in Fig. 1.

Eight 10-in.-beam finite elements with translations and rotations as structural degrees-of-freedom (DOF's) are used to model the vertical beam. The crosspiece is symmetrical relative to the vertical beam, and only symmetrical out-of-plane motion of the crosspiece is represented in the modeling. The flexible portion of the crosspiece is modeled as a two-DOF spring-mass system, as shown in Fig. 2. A string-in-tension finite element represents each cable. The model includes geometric stiffness matrices accounting for tension in the beam elements. Small lumped masses representing the control system coils, cable clamps, and the crosspiece clamp are added to the model. Inherent damping is not included in the analysis because it is small in comparison with the active damping imposed by the controller. Complete details of the modeling are given in Ref. 15.

The six lowest modes of the cruciform beam are of primary interest. Their calculated and measured natural frequencies and calculated mode shapes are shown in Fig. 2.

Active damping is effected by rate feedback control involving three force actuators, each colocated with a velocity sensor. The instantaneous control force at each actuator location is directly proportional, but opposite in sign, to the instantaneous velocity. This is equivalent to the attachment of a viscous dashpot to the structural DOF of the sensor, with the ratio of controlling force to sensed velocity being the viscous damping coefficient c_i.

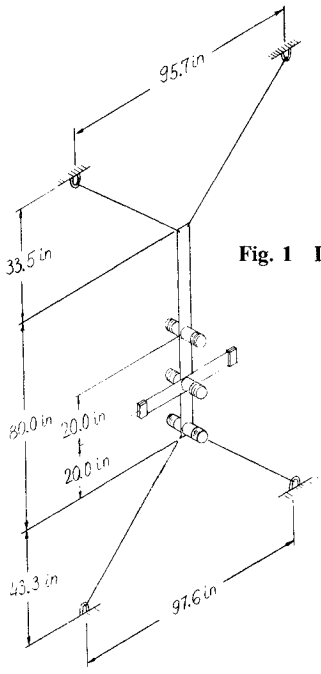

Fig. 1 Drawing of the laboratory structure.

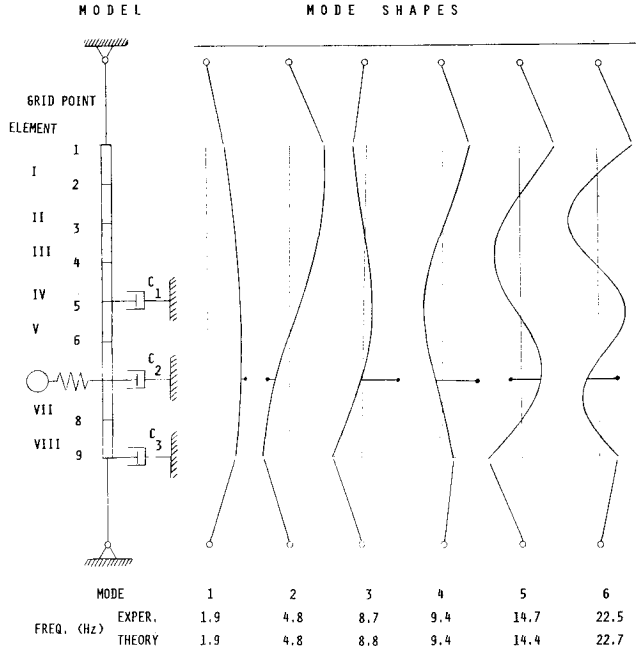

Fig. 2 Finite-element model and mode shapes.

The finite-element equations of motion may be written as $M\ddot{u} + C\dot{u} + Ku = 0$, where M, C, and K are the mass, damping, and stiffness matrices, and u is the displacement vector. The control system defines the C matrix, and, when the sensor-actuator pairs are located at grid points of the model, the C matrix consists only of diagonal elements equal to the c_i.

V. Theoretical Results and Discussion

The control system was designed for the cruciform beam so as to minimize the sum of the c_i supplied by the three actuators. The design variables were the values of individual c_i and the locations of the sensor-actuator pairs. The requirements imposed on the control system were $\zeta_j \geqq 0.03$ for the first six modes, $j = 1, \ldots, 6$. The optimization problem, Eq. (5), was solved by using a general-purpose software package—NEWSUMT.[16] NEWSUMT is based on a penalty function approach, which transforms the constrained optimization problem into a sequence of unconstrained problems. An extended interior penalty function is used, together with Newton's method, for solving the unconstrained problems. The control optimization procedure produced the baseline design $[x^*(p_0)]$ shown in Table 1, with the sensor-actuator locations almost exactly at grid points 5, 7, and 9. The fourth, fifth, and sixth damping ratios $(\zeta_4, \zeta_5, \zeta_6)$ were at the lower limit of 0.03, whereas the first three damping ratios were above this value.

Next, the structural design parameter vector p was chosen to represent small additional masses m_k at the nine grid points of the finite-element model. This choice was motivated by the ease of implementing the change experimentally. The robustness type sensitivity $[\partial g_j/\partial m_k(x^*, p_0)]$ was calculated by computing the derivatives of the three critical damping ratios $(\partial\zeta_4/\partial m_k, \partial\zeta_5/\partial m_k, \partial\zeta_6/\partial m_k)$ with respect to the additional mass. The results are presented in Table 2, normalized to show the expected change in damping ratios $\Delta\zeta_j$ effected by adding a concentrated mass m_k that is 1% of the total mass of the structure. The results in Table 2 indicate that adding the small mass at grid point 1 can reduce ζ_4 from 0.03 to 0.02, so that the control system is not at all robust.

Table 1 Controller gains c_i [lb-s/in. (N-s/m)] and performance index $(c_1 + c_2 + c_3)$ for all designs

Gain[a]	Uniform gain design	Baseline design	Added mass (node 8) design
c_1	0.01188 (2.0805)	0.06289 (11.0137)	0.06248 (10.9419)
c_2	0.01188 (2.0805)	0.01165 (2.0402)	0.00000 (0.0000)
c_3	0.01188 (2.0805)	0.02870 (5.0261)	0.03272 (5.7301)
Σc_i	0.03564 (6.2415)	0.10324 (18.0800)	0.09520 (16.6720)

[a]With sensor-actuator pairs located at grid points 5, 7, and 9.

Table 2 Change in damping ratios for three critical modes due to a concentrated mass equal to 1% of mass of the structure

Grid point location of mass	$\Delta\zeta_4$	$\Delta\zeta_5$	$\Delta\zeta_6$
1	−0.0100	−0.0090	0.0018
2	−0.0033	0.0002	−0.0003
3	0.0000	−0.0009	0.0014
4	−0.0021	−0.0004	−0.0004
5	−0.0055	0.0003	−0.0020
6	−0.0044	−0.0003	−0.0005
7	−0.0007	0.0007	−0.0002
8	0.0016	0.0000	0.0001
9	0.0026	−0.0029	−0.0015

Table 3 Sensitivity of the minimum sum of control gains with respect to added masses for the baseline design [lb-s/in. (N-s/m)]

Grid point location of mass	$\Delta(\Sigma c_i)^*$ for $m_k = 0.00022236$ lb-s^2/in. (0.03894 kg) (1% of mass of structure)	
1	0.02395	(4.1943)
2	0.00745	(1.3047)
3	0.00124	(0.2172)
4	0.00585	(1.0245)
5	0.01347	(2.3590)
6	0.01141	(1.9982)
7	−0.00011	(−0.0193)
8	−0.00402	(−0.7040)
9	0.00285	(0.4991)

Next, the optimum sensitivity calculations ($\partial f^*/\partial m_k$) were performed. Here Eq. (2) becomes

$$\frac{\partial f^*}{\partial m_k} = -\sum_{j=1}^{6} \lambda_j \frac{\partial g_j}{\partial m_k} = -\sum_{j=1}^{6} \lambda_j \frac{\partial \zeta_j}{\partial m_k} \qquad (6)$$

The sensitivity of the objective function to the additional 1% mass $[\Delta(\Sigma c_i)^* = (\partial f^*/\partial m_k) m_k]$ is given in Table 3. It shows that an additional mass at grid point 1 has the most detrimental effect, increasing the objective function by 23%, whereas an added mass at grid point 8 has the most beneficial effect, reducing the objective function by 3.9%.

The results of the sensitivity predictions were checked by redesigning the control system for a modified structure. A mass corresponding to 0.86% of the total mass of the structure was added at grid point 1. Table 4 compares the sensitivity analysis predictions to results obtained by reoptimizing the control system for the modified structure. The agreement between the sensitivity predictions and the reoptimized results is very good.

In enhancing the control system performance, the sensitivity calculation $\partial x^*/\partial m_k$ showed that the gain of the second actuator is reduced as the mass is added to grid point 8. The mass that was added to this grid point was chosen to make this gain equal to zero and corresponds to 2.0% of the total mass of the structure. It is predicted to improve the objective function by 7.7% (see Table 1). Increasing the mass further is not helpful because the gain of the second actuator cannot be reduced below zero. However, the improvement of 7.7% is considered to be substantial for such a minor change in the mass.

These results indicate that the potential for harmful interaction is very large, but there is also a significant potential for beneficial interaction. Thus, the results indicate that for this case simultaneous structures/control design may be indicated.

VI. Experimental Apparatus and Procedure

Experiments were conducted to test the accuracy of theoretical predictions against laboratory measurements. Four cases were tested in the experimental study with the use of the control gains given in Table 1. First, an unoptimized control design consisting of the uniform gains given in Table 1 was tested to validate the theoretical model before any optimization was performed. Second, the baseline case was tested. Third, the baseline design with an added mass at grid point 1 was tested to check predictions of robustness. Fourth, the design with an added mass at grid point 8 was tested. Displacement frequency response functions were measured at four positions on the vertical beam, and values for ζ_r and ω_r were inferred from the data for comparison with theoretical predictions.

The basic experimental apparatus and procedures are described in detail in Refs. 7 and 15. A summary of the apparatus used and the procedure relevant to this paper is provided here. Figure 3 is a photograph of part of the structure showing the three sensor-actuator pairs with the supporting framework. Figure 4 is a photograph showing the crosspiece and sensor-actuator pair located at grid point 7.

The added mass consisted of a small ceramic magnet and other small pieces of magnetic metal. The magnet and other metallic pieces were held firmly to the steel beam by the magnetic field. The added mass was placed on one side of the beam at grid point 1 or 8. The rotational inertia of the added mass was negligible and was not included in the theoretical model. The small additional beam and cable tensions caused by the added mass were also negligible.

Detailed descriptions of the control and instrumentation systems are given in Refs. 7 and 15. The three colocated sensor-actuator pairs, along with an analog feedback gain

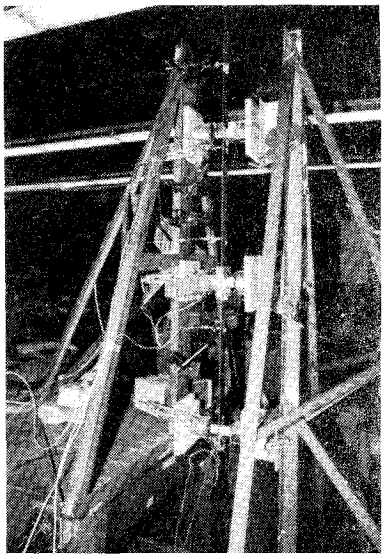

Fig. 3 Photograph of part of the structure with sensor-actuator pairs and supporting framework.

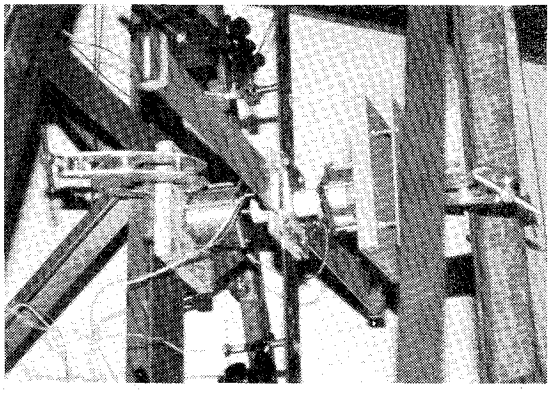

Fig. 4 Photograph of the crosspiece and sensor-actuator pair located at grid point 7.

Table 4 Comparison between sensitivity analysis prediction results and reoptimization for 0.86% added mass (at grid point 1) design [lb-s/in. (N-s/m)]

Gain	Sensitivity analysis from Eq. (1)	By reoptimization
c_1	0.05735 (10.0435)	0.05779 (10.1206)
c_2	0.04992 (8.7423)	0.05185 (9.0803)
c_3	0.01663 (2.9123)	0.01595 (2.7933)
Σc_i	0.12390 (21.6981)	0.12559 (21.9942)

Table 5 Repeatability of measured modal damping ratios for the baseline design

	Test number		
Mode	1	2	3
1	0.214	0.194	0.192
2	0.043	0.039	0.039
3	0.051	0.050	0.050
4	0.032	0.034	0.041
5	0.024	0.024	0.023
6	0.033	0.025	0.028

circuit and a controlled-current power amplifier for each sensor-actuator pair, made up the control system. Noncontacting velocity sensors produced voltage proportional to the velocity, and noncontacting force actuators generated force proportional to the control feedback signal. Each device consisted of a conducting coil attached to the beam and a magnetic field structure attached to the supporting framework (Fig. 5). An STI-11/23 data-acquisition and analysis system developed by Synergistic Technology Inc. of Cupertino, California, generated the excitation signal, acquired all of the response and excitation signals, and performed all data analysis. The excitation signal was added to the control feedback signal for grid point 9, so that one actuator coil served the dual purpose of control actuator and exciter. The relationship of the control system parameters to the theoretical viscous damping constant is developed in Ref. 7.

Translation-to-force frequency response functions (FRF) were measured at four locations on the vertical beam. The translation sensors used were noncontacting inductive-type proximity probes. Some of these proximity probes can be seen in Fig. 4 in the mounted positions. Random excitation was used. To achieve a good signal-to-noise ratio, the general excitation level was set as high as possible, consistent with maintaining linear behavior of the proximity probes, velocity sensors, and force actuators. Fast Fourier transforms of the response and excitation signals were calculated, and the former were divided by the latter to produce four FRF's. The frequency resolution was 0.0781 Hz. In all cases, the FRF's calculated from a single excitation period without data windowing were reasonably smooth and repeatable, so that the experimental spectral data were neither averaged nor windowed. The repeatability was tested by performing each experiment three times and comparing the results.

VII. Experimental Results and Comparison with Theory

A representative FRF is plotted in Fig. 6. The solid curve is experimentally measured data for the added mass design, and the dashed curve is a curve fit to the experimental data calculated by the STI-VAMP (Version 5A) software. The curve fitting was based on a six-mode theoretical model, where the frequencies and damping ratios were calculated for each of the four FRF's and then global averages were calculated. The curve fit is clearly very good, with no significant deviations from the experimental data.

Each of the four cases tested experimentally was repeated twice. Table 5 illustrates for the baseline design the good repeatability of modal damping factors calculated from experimental data. The results for the other designs were comparably repeatable.

The prediction that a small mass at grid point 1 has a large detrimental effect on the performance of the system was checked by adding 1.31% of the total mass of the structure at that location. The choice of the magnitude of the mass was based on convenience in the experimental verification. Table 6 compares the analytical predictions and experimental measurement of the effects of the added mass. There are substantial differences between predictions and measurements for the

Table 6 Theoretical and experimental modal damping ratios for 1.31% added mass design (at grid point 1)

Mode	Theory	Experiment
1	0.218	0.187
2	0.043	0.038
3	0.085	0.059
4	0.017	0.020
5	0.029	0.021
6	0.032	0.031

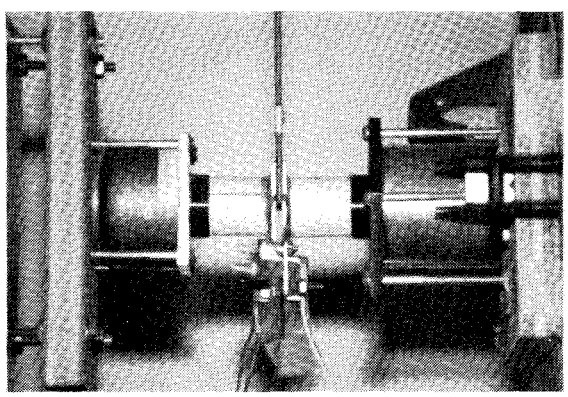

Fig. 5 Closeup photograph of sensor (at right) and actuator (at left) at grid point 9.

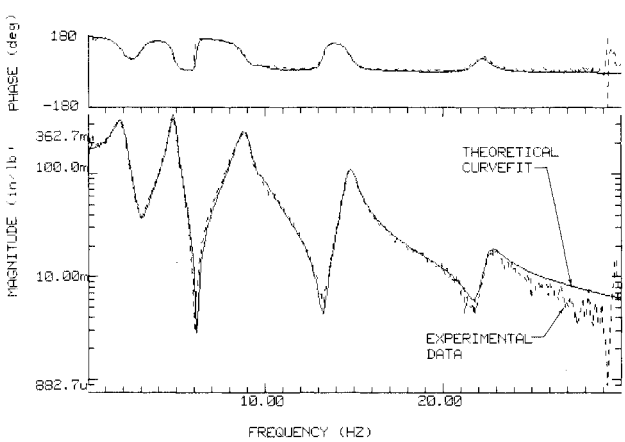

Fig. 6 Translation-to-force FRF of response 2 in. above grid point 9 due to excitation at grid point 9, for the baseline control system.

Table 7 Theoretical and experimental modal damping factors

	Uniform gain design		Baseline design		2.0% added mass (at grid point 8) design	
Mode	Theory	Experiment[a]	Theory	Experiment[a]	Theory	Experiment[a]
1	0.074	0.068 (1.3)	0.219	0.200 (6.1)	0.194	0.170 (0.7)
2	0.018	0.017 (6.2)	0.046	0.040 (5.7)	0.047	0.041 (1.4)
3	0.022	0.024 (9.7)	0.071	0.050 (1.1)	0.074	0.062 (7.6)
4	0.010	0.010 (4.6)	0.030	0.036 (13.3)	0.030	0.034 (10.5)
5	0.013	0.013 (6.6)	0.030	0.024 (1.9)	0.030	0.022 (0.7)
6	0.008	0.007 (3.5)	0.030	0.029 (14.0)	0.030	0.028 (5.5)

[a]The experimental modal damping factor presented is the average of three separate measurements. The value given in parentheses is the percent of the standard deviation of those three measurements relative to the average.

third and fifth modes, but in general the agreement is good. In particular, it is clear that the additional mass severely reduces the damping ratio for the fourth mode, as predicted by the analysis. These results validate the theoretical prediction of the large detrimental effect of a small mass on the performance of the control system.

Table 7 compares the analytical predictions and experimental measurements for the other three designs. The agreement is very good for the uniform-gain design and fairly good for the other two designs. The poorer agreement of the optimized designs may be expected because the optimization process tends to capitalize on second-order effects that are more poorly modeled. However, the agreement is close enough to validate the analytical predictions.

Acknowledgment

The research reported in this paper was supported in part by NASA Grant NAG-1-224.

References

[1]Messac, A. and Turner, J., "Dual Structural Control Optimization of Large Space Structures," AIAA Paper 84-1044-CP, Palm Springs, CA, May 1984.

[2]Hale, A.L., Lisowski, R.J., and Dahl, W.L., "Optimal Simultaneous Structural and Control Design of Maneuvering Flexible Spacecraft," *Journal of Guidance, Control, and Dynamics*, Vol. 8, Jan.-Feb. 1985, pp. 86-93.

[3]Salama, M., Hamidi, M., and Demsetz, L., "Optimization of Controlled Structures," *Proceedings of the JPL Workshop on Identification and Control of Flexible Space Structures*, Jet Propulsion Lab., Publ. 85-29, Vol. II, April 1985, pp. 311-327.

[4]Hanks, B.R. and Skelton, R.E., "Designing Structures for Reduced Response by Modern Control Theory," *Proceedings of the AIAA 24th Structures, Structural Dynamics, and Materials Conference*, Lake Tahoe, NV, May, 1983.

[5]Khot, N.S., Venkayya, V.B., and Eastep, F.E., "Structural Modifications to Reduce the LOS-Error in Large Space Structures," AIAA Paper 84-0997, May 1984.

[6]Khot, N.S. and Venkayya, V.B., "Structural Modifications of Large Flexible Structures to Improve Controllability," AIAA Paper 84-1906, Aug. 1984.

[7]Haftka, R.T., Martinovic, Z.N., and Hallauer, W.L., Jr., "Enhanced Vibration Controllability by Minor Structural Modification," AIAA Paper 84-1036, May 1984; also *AIAA Journal*, Vol. 23, Aug. 1985, pp. 1260-1266.

[8]Kammer, D.C. and Sesak, J.R., "Actuator Number Versus Parameter Sensitivity in Flexible Spacecraft Control," *Second VPI& SU/AIAA Symposium on Dynamics and Control of Large Flexible Spacecraft*, Blacksburg, VA, 1979.

[9]Yedavalli, R.K. and Skelton, R.E., "Determination of Critical Parameters in Large Flexible Space Structures with Uncertain Modal Data," *ASME Journal of Dynamic Systems, Measurement, and Control*, Vol. 105, Dec. 1983, pp. 238-244.

[10]Yedavalli, R.K., "Critical Parameter Selection in the Vibration Suppression of Large Space Structures," *Journal of Guidance, Control, and Dynamics*, Vol. 7, May-June 1984, pp. 274-278.

[11]Haftka, R.T. and Kamat, M.P., *Elements of Structural Optimization*, Martinus Nijhoff, The Netherlands, 1985, pp. 181-183.

[12]Bauldry, R.D., Breakwell, J.A., Chambers, G.J., Johansen, K.F., Nguyen, N.C., and Schaechter, D.B., "A Hardware Demonstration of Control for a Flexible Offset-Feed Antenna," *Journal of the Astronautical Sciences*, Vol. 21, No. 3, July-Sept. 1983, pp. 455-470.

[13]Aubrun, J.N., Ratner, M.J., and Lyons, M.G., "Structural Control for a Circular Plate," *Journal of Guidance, Control, and Dynamics*, Vol. 7, Sept.-Oct. 1984, pp. 535-545.

[14]Horner, G.C., "Optimum Actuator Placement, Gain, and Number for a Two-Dimensional Grillage," *Proceedings of the AIAA 24th Structures, Structural Dynamics, and Material Conference*, Lake Tahoe, NV, May 1983, Pt. 2, pp. 179-192.

[15]Schamel, G.C., "Active Damping of a Structure with Low Frequency and Closely Spaced Modes: Experiments and Theory," M.S. Thesis, Virginia Polytechnic Inst. and State Univ., Blacksburg, VA, March 1985.

[16]Miura, H. and Schmit, L.A., "NEWSUMT—A Fortran Program for Inequality Constrained Function Minimization—Users Guide," NASA CR-159070, June 1979.